Numerical evaluation of the slope and intercept of end-systolic pressure-volume relation

R. M. Shoucri
Department of Mathematics & Computer Science,
Royal Military College of Canada, Canada

Abstract

Numerical evaluation of two methods to calculate slope and intercept of end-systolic pressure-volume relation (ESPVR) in the left ventricle is presented. The mathematical formalism is based on results previously published in which the active force of the myocardium (also called isovolumic pressure P_{iso}) is introduced in the formalism describing the pressure-volume relation (PVR) in the left ventricle. The numerical calculation is simple and can be easily implemented in routine clinical work, only the ventricular pressure P_m near end-systole needs to be estimated. A thick-walled cylindrical model contracting symmetrically is assumed for the left ventricle.

Keywords: ventricular elastance, end-systolic pressure-volume relation, pressure-volume relation in the ventricles, peak isovolumic pressure, active force of the myocardium.

1 Introduction

In previous studies the author has stressed the importance of introducing the active force of the myocardium (also called isovolumic pressure P_{iso} by physiologists) in the formalism describing the pressure-volume relation (PVR) in the ventricles [1–5]. The mathematical formalism developed was used to calculate the stress in the myocardium by using linear elasticity [5] and large elastic deformation [1–4], in this formalism the active force of the myocardium is modelled as force/unit volume of the myocardium generated by the cardiac muscle (see fig. 1). In this study a relation derived in [2] is used to calculate the non-linear end-systolic pressure-volume relation (ESPVR). It is shown that this mathematical relation can be used to calculate in a non-invasive way the

WIT Transactions on Biomedicine and Health, Vol 15, © 2011 WIT Press
www.witpress.com, ISSN 1743-3525 (on-line)
doi:10.2495/EHR110291

intercept V_{om} of the ESPVR with the volume axis (see fig. 2), only knowledge of the volume of the myocardium V_{ω}, the end-systolic volume V_{ed} and the ventricular cavity volume V_m near end-systole are required in order to calculate V_{om}. If the ventricular cavity pressure P_m near end-systole can be estimated in a non-invasive way, then the different slopes of the non-linear ESPVR (see fig. 2) and the peak isovolumic pressure P_{isom} can also be calculated in a non-invasive way. This study focuses on a comparison between a numerical approximation obtained by assuming that for small z, $\log(1 + z) \approx z$, with the exact expression using the logarithmic function. The interest of this approximation is that the calculations are much simpler.

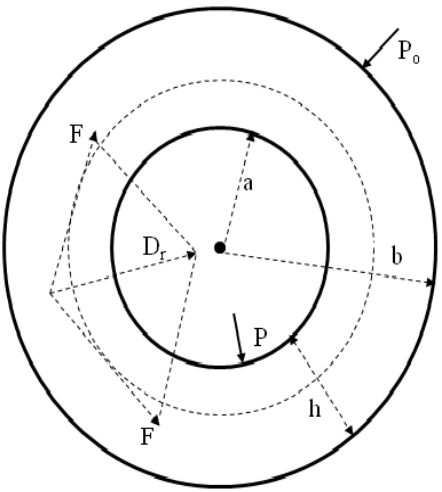

Figure 1: The left ventricle is represented as a thick-walled cylinder contracting symmetrically. P = ventricular pressure, P_o = outer pressure (neglected in the calculation), a = inner radius, b = outer radius, h = b – a = thickness of the myocardium. A helical fibre is projected on the cross-section as a dotted circle. Because of the assumed symmetry of the contraction, a radial active force $D_r(r)$ (force/unit volume of the myocardium) is generated by the muscular fibre.

Although the cardiac pressure-volume loops at different loadings appear to define an almost linear relationship of end systolic values, the ESPVR is essentially a non-linear relation (see references [6–8]). Several approaches have been proposed to estimate the parameters of the ESPVR from single beat measurement [9, 10] (for a critical review see [10]), but none has the simplicity of the method presented in this study.

2 Mathematical model

As in previous studies a quasi-static approximation of the ventricular contraction is considered (inertia forces and viscous forces neglected). Figure 1 shows a cross-section of the left ventricle that is modelled a thick-walled cylinder contracting symmetrically, a helical myocardial fibre is projected on the cross-section as a dotted circle. It will generate a radial active fore/unit volume of the myocardium $D_r(r)$, this force will develop an active pressure on the inner surface of the myocardium (endocardium) given by

$$\int_a^b D_r(r)\, dr = \bar{D}h \tag{1}$$

The thickness of the myocardium is given by h = b – a, a = inner radius of the myocardium, b = outer radius of the myocardium. $\bar{D}$ is an average radial force/unit volume of the myocardium calculated by applying the mean value theorem. We shall follow the practice of physiologists and by writing $\bar{D}h = P_{iso}$, where P_{iso} is the isovolumic pressure developed in a non-ejecting contraction. Near end-systole when the myocardium reaches its maximum state of activation, the equilibrium of forces on the inner surface of the myocardium in a quasi-static approximation can be written as follows

$$P_{isom} - P_m = E_{2mx}\,(V_{ed} - V_m) \tag{2}$$

The left hand side is the resultant pressure applied on the inner force of the myocardium. The right hand side is the pressure resulting from the change of volume from V_{ed} (end-diastole when dV/dt = 0) to V_m when the cardiac muscle reaches its maximum state of activation ($V_m \approx V_{es}$ the end-systolic volume when dV/dt = 0), the corresponding ventricular pressure is P_m. From fig. 2, one can deduce that the elasticity coefficient $E_{2mx} = \tan\beta_2$. The outer pressure P_o in fig. 1 is neglected.

If P_{isom} is kept constant and (P_m, V_m) is varied in eqn (2), then the point (P_m, V_m) will describe the ESPVR represented by the curve BDC in fig. 2, as if a balloon is inflated against a constant P_{isom}.

Equation (2) can be split into two equations as follows

$$P_m = E_{1mx}\,(V_m - V_{om}) \tag{3}$$

$$P_{isom} = E_{mx}\,(V_{ed} - V_{om}) \tag{4}$$

The intercept V_{om} of the non-linear ESPVR with the volume axis is shown in fig. 2. From fig. 2, one can deduce that the coefficients $E_{1mx} = \tan\beta_1$ and $E_{mx} = \tan\alpha$. An interesting feature of the preceding equations is the introduction of the peak isovolumic pressure P_{isom} in the formalism describing the ESPVR.

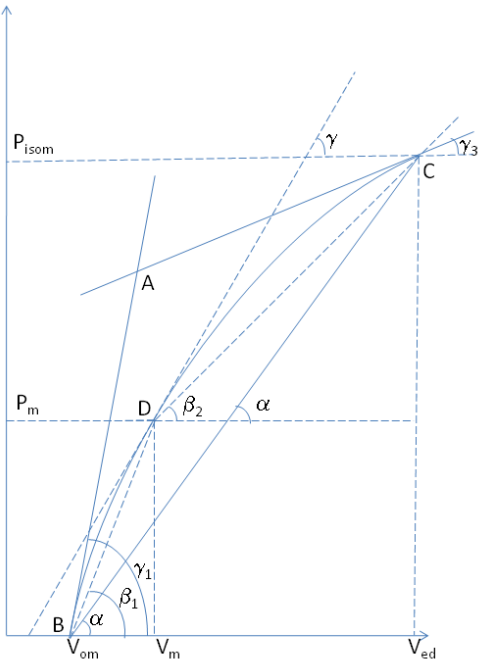

Figure 2: Non-linear ESPVR represented by the curve BDC, D has coordinates (P_m, V_m). P_m is the left ventricular pressure (corresponding to the maximum state of activation of the muscle), P_{isom} is the peak isovolumic pressure. E_{mx} = tanα slope of BC, E_{1mx} = tanβ_1 slope of BD, E_{2mx} = tanβ_2 slope of DC. The slope of the tangent to the ESPVR at D is tanγ.

3 Slopes of the ESPVR

Unlike the linear ESPVR that is characterized by one slope, we have in fig. 2 several slopes that characterize the non-linear ESPVR. These slopes are

$$tan\beta_2 = E_{2mx} = \text{slope of the line CD} \quad (5a)$$

$$tan\alpha = E_{mx} = \text{slope of the line CB} \quad (5b)$$

$$tan\beta_1 = E_{1mx} = \text{slope of the line DB} \quad (5c)$$

$$\tan \gamma = \frac{dP_m}{dV_m} = \text{tangent to the ESPVR BDC at point D } (P_m, V_m) \quad (5d)$$

$$tan\gamma_1 = \text{tangent to the ESPVR BDC at point B } (0, V_{om}) \quad (5e)$$

$$tan\gamma_3 = \text{tangent to the ESPVR BDC at point C } (P_{isom}, V_{ed}) \quad (5f)$$

We give in this section an exact expression of slopes based on the cylindrical model of the ventricular cavity as derived in [2], we then discuss in the next section the numerical calculation procedures.

a) From reference [2] we can write

$$tan\beta_2 = k_w \left(\frac{1}{V_m} - \frac{1}{V_m+V_\omega} + \frac{log\frac{V_m+V_\omega}{V_{ed}+V_\omega} - log\frac{V_m}{V_{ed}}}{V_{ed}-V_m}\right) \quad (6a)$$

We use log to represent the natural logarithm, k_w is a constant coefficient calculated by applying the mean value theorem in [2]. For small z we can apply the relation log (1 + z) ≈ z, we get the following approximate expression $tan\beta_{2a}$

$$tan\beta_{2a} \approx k_{wa} \left(\frac{1}{V_m} - \frac{1}{V_m+V_\omega} + \frac{1}{V_{ed}} - \frac{1}{V_{ed}+V_\omega}\right) \quad (6b)$$

The coefficient k_{wa} corresponds to the calculation carried out when the approximation log (1 + z) ≈ z is used.

b) When point D moves to point B, $V_m \rightarrow V_{om}$ and $tan\beta_2 \rightarrow tan\alpha$. We get

$$tan\alpha = k_w \left(\frac{1}{V_{om}} - \frac{1}{V_{om}+V_\omega} + \frac{log\frac{V_{om}+V_\omega}{V_{ed}+V_\omega} - log\frac{V_{om}}{V_{ed}}}{V_{ed}-V_{om}}\right) \quad (7a)$$

By applying the approximation log (1 + z) ≈ z we get the following approximate expression $tan\alpha_a$

$$tan\alpha_a \approx k_{wa} \left(\frac{1}{V_{om}} - \frac{1}{V_{om}+V_\omega} + \frac{1}{V_{ed}} - \frac{1}{V_{ed}+V_\omega}\right) \quad (7b)$$

c) From eqns (4) and (7a) one can derive the following expression for P_{isom}

$$P_{isom} = k_w \left[\left(\frac{1}{V_{om}} - \frac{1}{V_{om}+V_\omega}\right)(V_{ed} - V_{om}) + log\frac{V_{om}+V_\omega}{V_{ed}+V_\omega} - log\frac{V_{om}}{V_{ed}}\right] \quad (8a)$$

and the approximate expression P_{isoma}

$$P_{isoma} \approx k_{wa} \left(\frac{1}{V_{om}} - \frac{1}{V_{om}+V_\omega} + \frac{1}{V_{ed}} - \frac{1}{V_{ed}+V_\omega}\right)(V_{ed} - V_{om}) \quad (8b)$$

d) We note that $P_m = P_{isom} - (P_{isom} - P_m)$, which can be written as

$$P_m = tan\alpha\,(V_{ed} - V_{om}) - tan\beta_2\,(V_{ed} - V_m) \quad (9a)$$

By using eqns (6a) and (7a) we get

$$P_m = k_w \left[\left(\frac{1}{V_{om}} - \frac{1}{V_{om}+V_\omega}\right)(V_{ed} - V_{om}) - \left(\frac{1}{V_m} - \frac{1}{V_m+V_\omega}\right)(V_{ed} - V_m) + log\frac{V_{om}+V_\omega}{V_{ed}+V_\omega} - log\frac{V_{om}}{V_{ed}} - \left(log\frac{V_m+V_\omega}{V_{ed}+V_\omega} - log\frac{V_m}{V_{ed}}\right)\right] \quad (9b)$$

By combining the logarithmic terms, we get:

$$P_m = k_w \left[\left(\frac{1}{V_{om}} - \frac{1}{V_{om}+V_\omega}\right)(V_{ed} - V_{om}) - \left(\frac{1}{V_m} - \frac{1}{V_m+V_\omega}\right)(V_{ed} - V_m) + log\frac{V_{om}+V_\omega}{V_m+V_\omega} - log\frac{V_{om}}{V_m}\right] \quad (9c)$$

We notice that by using the approximation log (1 + z) ≈ z when z is small, eqns (9b) and (9c) give different results. We use eqn (9c) to obtain the approximation

$$P_{ma} \approx k_{wa}\left[\left(\frac{1}{V_{om}} - \frac{1}{V_{om}+V_{\omega}}\right)(V_{ed} - V_{om}) - \left(\frac{1}{V_m} - \frac{1}{V_m+V_{\omega}}\right)(V_{ed} - V_m) + \left(\frac{1}{V_m} - \frac{1}{V_m+V_{\omega}}\right)(V_m - V_{om})\right] \quad (9d)$$

e) The slope $\tan\beta_1 = E_{1mx}$ is calculated from eqn (3) and eqn (9a), we get

$$tan\beta_1 = \frac{P_m}{V_m - V_{om}} \quad (10a)$$

$$tan\beta_1 = \frac{tan\alpha\,(V_{ed} - V_{om}) - tan\beta_2\,(V_{ed} - V_m)}{V_m - V_{om}} \quad (10b)$$

By using eqn (9c) we get

$$tan\beta_1 = k_w\left[\left(\frac{1}{V_{om}} - \frac{1}{V_{om}+V_{\omega}}\right)\frac{V_{ed} - V_{om}}{V_m - V_{om}} - \left(\frac{1}{V_m} - \frac{1}{V_m+V_{\omega}}\right)\frac{V_{ed} - V_m}{V_m - V_{om}} + \frac{log\frac{V_{om}+V_{\omega}}{V_m+V_{\omega}} - log\frac{V_{om}}{V_m}}{V_m - V_{om}}\right] \quad (10c)$$

By using the approximation log (1 + z) ≈ z for small z, we obtain the approximation

$$tan\beta_{1a} \approx \frac{1}{V_{om}} - \frac{1}{V_{om}+V_{\omega}} + \frac{1}{V_m} - \frac{1}{V_m+V_{\omega}} + k_{wa}\left[\frac{1}{V_{om}} - \frac{1}{V_{om}+V_{\omega}} - \left(\frac{1}{V_m} - \frac{1}{V_m+V_{\omega}}\right)\right]\frac{V_{ed} - V_m}{V_m - V_{om}} \quad (10d)$$

f) In order to calculate the tangent to the ESPVR (see eqn (5d)), we calculate the derivative dP_m/dV_m from eqn (9c) to obtain

$$tan\gamma = k_w\left[2\left(\frac{1}{V_m} - \frac{1}{V_m+V_{\omega}}\right) + \left(\frac{1}{V_m} - \frac{1}{V_m+V_{\omega}}\right)\left(\frac{1}{V_m} + \frac{1}{V_m+V_{\omega}}\right)(V_{ed} - V_m)\right] \quad (11)$$

g) We obtain $\tan\gamma_1$ (see eqn (5e)) by letting $V_m \rightarrow V_{om}$ in eqn (11), we get

$$tan\gamma_1 = k_w\left[2\left(\frac{1}{V_{om}} - \frac{1}{V_{om}+V_{\omega}}\right) + \left(\frac{1}{V_{om}} - \frac{1}{V_{om}+V_{\omega}}\right)\left(\frac{1}{V_{om}} + \frac{1}{V_{om}+V_{\omega}}\right)(V_{ed} - V_{om})\right] \quad (12)$$

We obtain $\tan\gamma_3$ (see eqn. (5f)) by letting $V_m \rightarrow V_{ed}$ in eqn. (11), we get

$$tan\gamma_3 = k_w\left[2\left(\frac{1}{V_{ed}} - \frac{1}{V_{ed}+V_{\omega}}\right)\right] \quad (13)$$

4 Numerical application

The numerical application is based on the experimental data published by Burns et al. [11] for experiments on dogs. The values of V_{ed}, $V_{es} \approx V_m$, V_{ω} are given in [11] as well as the maximum left ventricular pressure P_{max}. We have assumed that the pressure P_m near end-systole, corresponding to the maximum state of

activation of the muscle, can be estimated from $P_m \approx P_{max}/1.2$ approximately. These values are shown in Table 1.

Table 1: Result of the calculation of V_{om} and P_{isom} by two different methods.

					Exact		Approximate	
	P_{max} mmHg	mass gr.	V_{ed} ml	V_m ml	P_{isom} mmHg	V_{om} ml	P_{isom} mmHg	V_{om} ml
1	113	73	17.7	5.6	191.92	3.18	180.78	3.34
2	144		30.3	4.7	241.84	2.44	231.09	2.57
3	144		49.2	8.0	239.30	4.21	227.81	4.43
4	109	136.4	23.8	9.7	186.04	5.86	175.30	6.11
5	139		41.0	19.7	233.76	12.61	219.47	13.05
6	155		56.5	27.2	258.56	17.51	241.94	18.11
7	103	91.4	34.3	27.0	171.36	22.16	165.04	22.34
8	142		49.9	38.1	234.85	30.72	224.72	31.01
9	155		63.3	50.4	255.80	41.84	245.53	42.15
10	115	123	24.5	11.4	195.41	7.19	184.09	7.45
11	133		49.5	40.6	221.07	34.31	213.89	34.51
12	135	138.8	38.5	23.8	226.67	16.93	214.68	17.31
13	149		52.3	29.6	248.74	20.28	233.93	20.82
14	153		70.0	29.7	254.08	18.42	237.03	19.14
15	101	155.9	56.2	34.0	168.68	24.00	159.17	24.55
16	150.4		87.0	55.9	248.39	40.88	234.06	41.66

end-systolic pressure P_m = max. pressure $P_{max}/1.2$; myocardial volume in ml V_ω = mass/density, density = 1.055 g/cm^3; data for P_{max}, mass, V_{ed} and V_m taken from Burns et al. [11].

4.1 Calculation of V_{om}

The intercept V_{om} with the volume axis of the nonlinear ESPVR can be calculated from the three following approximate relations. At point B (coordinates (0, V_{om})) on the ESPVR (see fig. 2) we have

$$tan\beta_1 \approx (tan\gamma_1 + tan\alpha)/2 \tag{14}$$

At point D (coordinates (P_m,V_m)) (see Fig. 2) we have

$$tan\gamma \approx (tan\beta_1 + tan\beta_2)/2 \tag{15}$$

At point C (coordinates (V_{ed}, P_{isom})) (see Fig. 2) we have

$$tan\beta_2 \approx (tan\gamma_3 + tan\alpha)/2 \tag{16}$$

It should be noticed that k_w simplifies on both sides of eqns. (14) to (16), so that only V_{ed}, $V_m \approx V_{es}$, and V_ω are needed to calculate V_{om}. The calculation is done by using Newton-Raphson method (see Appendix). It has been verified that

the three equations give the same result for V_{om}. Figure 3 shows the result of calculating V_{om} by using eqn (16) with the exact expressions (eqns (6a), (7a) and (13)), and the approximate expressions (eqns (6b), (7b) and (13)), the maximum error between the two approaches is of the order of 5.5%.

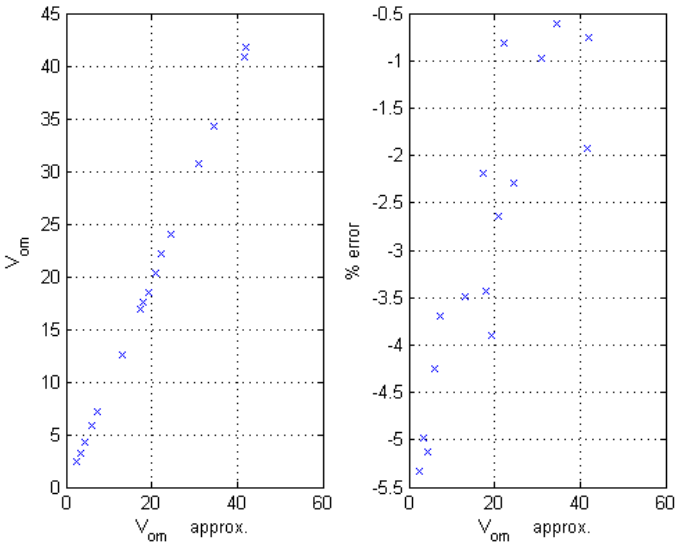

Figure 3: V_{om} (ml) is the intercept of the ESPVR with the volume axis, calculation of V_{om} is done by using the approximate relation $\log(1+z) \approx z$ (horizontal axis), and without using this approximation (vertical axis). The percentage relative error is shown on the right side (vertical axis).

4.2 Calculation of the coefficient k_w

The values of V_{ed}, $V_m \approx V_{es}$, V_ω,V_{om} and P_m are needed to calculate the coefficient k_w from eqns (9c) and (9d), the results are shown in fig. 4. The maximum relative error, due to the approximation $\log(1 + z) \approx z$, for the calculation of k_w is of the order of 17% (see fig. 4).

4.3 Calculation of the tangents

Because of space consideration only the results of the calculation of the tangents $\tan\beta_1$ and $\tan\gamma$ are shown in figs. 5 and 6. On the horizontal axis we have the results obtained by using the approximation $\log(1 + z) \approx z$, on the vertical axis we have the results obtained without using this approximation. The right hand side shows that the maximum error in all these cases is of the order of 10%.

The results for $\tan\alpha$ and $\tan\beta_2$ are similar.

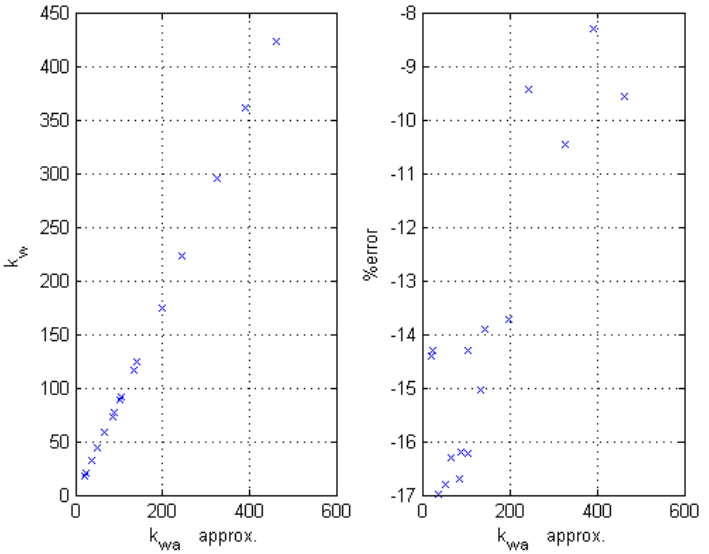

Figure 4: The coefficient k_w (mmHg) is calculated by using eqn (9d) (horizontal axis), and by using eqn (9c) (vertical axis); % error = $100*(k_w - k_{wa})/k_w$ is shown on the right side (vertical axis).

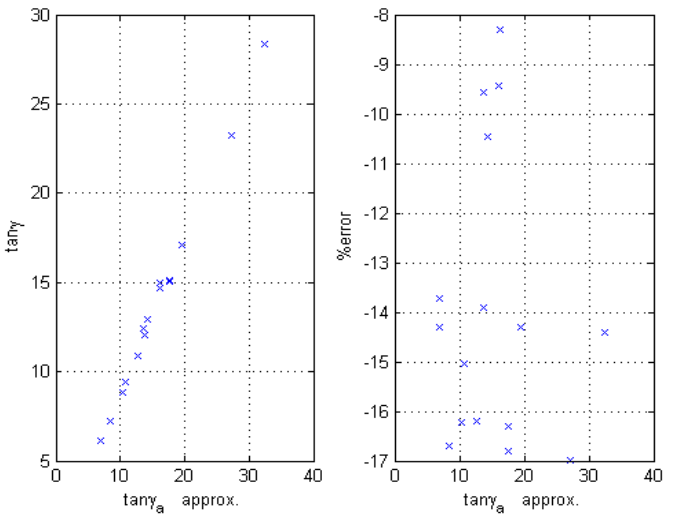

Figure 5: The tangent tanγ is calculated by using eqn (6b) (horizontal axis), and by using eqn (6a) (vertical axis); % error = $100*(tan\gamma - tan\gamma_a)/tan\gamma$ is shown on the right side (vertical axis).

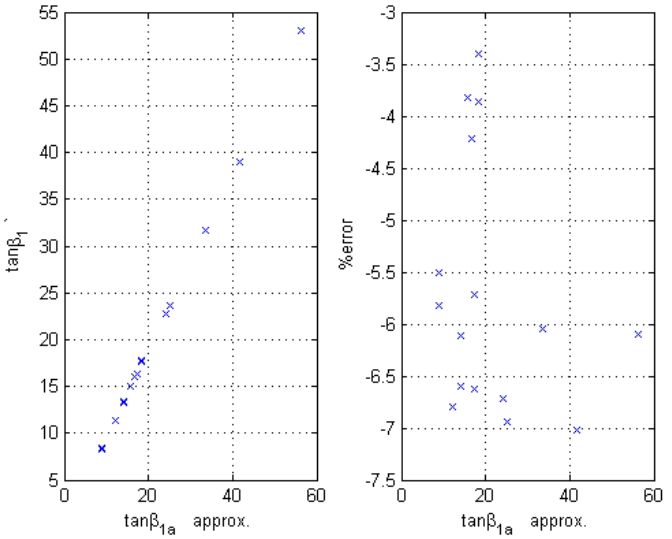

Figure 6: The slope $\tan\beta_1$ is calculated by using the approximate eqn (10d) (horizontal axis), and by using eqn (10c) (vertical axis); % error = $100*(\tan\beta_1 - \tan\beta_{1a})/\tan\beta_1$ is shown on the right side (vertical axis).

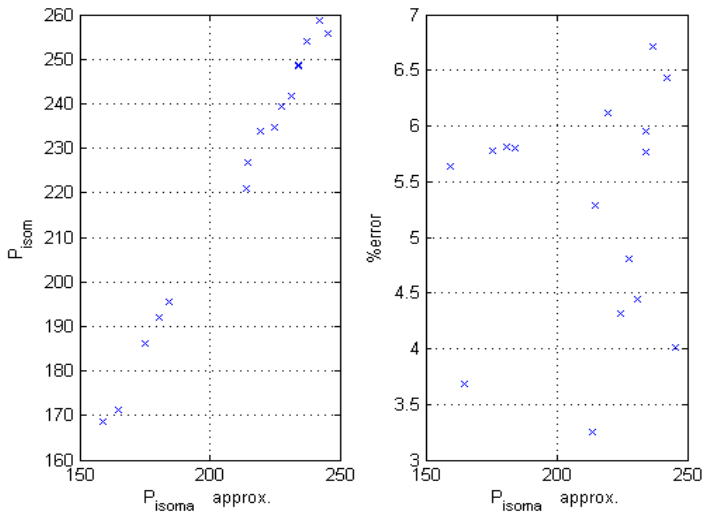

Figure 7: The peak isovolumic pressure P_{isom} (mmHg) is calculated by using the approximate eqn (8b) (horizontal axis), and by using eqn (8a) (vertical axis); % error = $100*(P_{isom} - P_{isoma})/P_{isom}$ is shown on the right side (vertical axis).

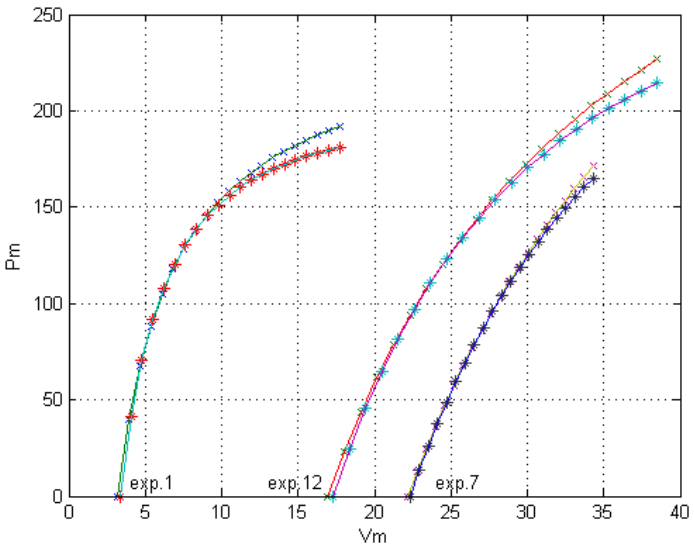

Figure 8: Variation of (P_m, V_m) along ESPVR using exact formula x (eqn. 9c) and approximate formula * (eqn. 9d) for three experiments taken from Table 1.

4.4 Calculation of P_{isom}

The calculation of the peak isovolumic pressure P_{isom} by using eqns (8a) and (8b) is shown in fig. 7. The maximum relative error in using the approximation $\log(1 + z) \approx z$ for the calculation of P_{isom} is of the order of 7%.

4.5 ESPVR

The calculation of the ESPVR was done by using eqns. (9), eqn. (2) can be used to verify the results. In the calculation of Fig. 8, V_m is varied from V_{om} to V_{ed} and P_m is calculated by using eqn (9c) for the exact value (x) and eqn (9d) for the approximate value (*) corresponding to the approximation $\log(1 + z) \approx z$. From Table 1 we see that we have

V_m varies from V_{om} = 3.34 ml to V_{ed} = 17.7 ml for experiment 1.
V_m varies from V_{om} = 22.34 ml to V_{ed} = 34.3 ml for experiment 7.
V_m varies from V_{om} = 17.31 ml to V_{ed} = 38.5 ml for experiment 12.

Only the results for three experiments are shown in a way not to overload the figure. The results of Fig. 8 show that the volume intercept V_{om} is not very much affected by the approximation $\log(1+z) \approx z$, and similarly for the peak isovolumic pressure P_{isom}.

5 Conclusion

We have investigated the possibility to use the approximation log(1 + z) ≈ z for small z in the calculation of different parameters used to describe the non-linear ESPVR. The result of this study indicates that this approximation seems to have small effect on the calculation of V_{om} or P_{isom}, but the error in the calculation of the slope to the ESPVR is relatively larger.

Appendix

The Newton-Raphson Method is used to solve Equation (16). By using the approximation log(1 + z) ≈ z we get

$$1 - \frac{V_m(V_m+V_\omega)}{V_{ed}(V_{ed}+V_\omega)} = \frac{V_m(V_m+V_\omega)}{V_o(V_o+V_\omega)} - 1 \tag{A1}$$

By writing

$$x = \frac{V_o}{V_m} \qquad y = \frac{V_o+V_\omega}{V_m+V_\omega} \tag{A2}$$

then eqn. (A1) can be written in the form

$$f(x,y) = \left[2 - \frac{V_m(V_m+V_\omega)}{V_{ed}(V_{ed}+V_\omega)}\right] x\, y - 1 \tag{A3}$$

The two eqns (A2) combine to give

$$g(x,y) = y\frac{V_m+V_\omega}{V_\omega} - x\,\frac{V_m}{V_\omega} - 1 \tag{A4}$$

We start with an approximation xo and yo to the solution of Eqs A3 & A4. A new approximation xn, yn is calculated from the relation

$$\begin{bmatrix} xn \\ yn \end{bmatrix} = \begin{bmatrix} xo \\ yo \end{bmatrix} - J^{-1}\begin{bmatrix} f(xo,yo) \\ g(xo,yo) \end{bmatrix}, \quad \text{with} \quad J = \begin{bmatrix} \frac{\partial f}{\partial x} & \frac{\partial f}{\partial y} \\ \frac{\partial g}{\partial x} & \frac{\partial g}{\partial y} \end{bmatrix} \tag{A5}$$

J^{-1} is the inverse of J. The MATLAB code is shown below, one can verify that the calculated values vom1 and vom2 representing V_{om} are equal.

```
function [vom1,vom2] = Calcul3Vo(ved,vm,vw)
%  ved = end-diastolic volume;  vm = end-systolic ventricular  volume
%  vw = volume of the myocardium;  xo, yo initial approximations
xo = 2/vm;   yo = (xo*vm  + vw)/(vm  +  vw);
epsx = 1.0;   epsy = 1.0;   count = 0;
while ((epsx >0.001) || (epsy >0.001))
Ko = 2 - (vm/ved)*(vm + vw)/(ved + vw);
fxy = Ko*xo*yo - 1;
gxy = yo*((vm + vw)/vw) - (vm/vw)*xo -1;
dfx = Ko*yo;    dfy = Ko*xo;
dgx = - vm/vw;    dgy = (vm + vw)/vw;
dlt = dfx*dgy - dfy*dgx;
```

```
xn = xo - (dgy*fxy - dfy*gxy)/dlt;
yn = yo - (-dgx*fxy + dfx*gxy)/dlt;
epsx = abs(xn - xo);  epsy = abs(yn - yo);
xo = xn;  yo = yn;
count = count + 1;
if (count > 15)
epsx = 0; epsy = 0;
end
end
vom1 = xo*vm;  vom2 = yo*(vm + vw) - vw;
```

References

[1] Shoucri, R.M., The pressure-volume relation and the mechanics of left ventricular contraction, *Japanese Heart Journal*, **31**, pp. 713-729, 1990.

[2] Shoucri, R.M., Theoretical study of pressure-volume relation in left ventricle,*Am. J. Physiol Heart Circ. Physiol.*, **260**, pp. H282-H291, 1991.

[3] Shoucri, R.M., Studying the mechanics of left ventricular contraction, *IEEE Engineering in Medicine and Biology Magazine*, **17**, pp. 95-101, May/June 1998.

[4] Shoucri, R.M.,Mathematical aspects of the mechanics of left ventricular contraction, *Int. J. of Design & Nature and Ecodynamics,* **5**, pp. 1-16, 2010.

[5] Shoucri, R.M., Comparison between linear elasticity and large elastic deformation in the study of the contraction of the myocardium, *Modelling in Medicine and Biology VII*, ed. C.A. Brebbia, WIT Press: Southampton & Boston, pp. 3-13, 2007.

[6] Kass, D.A., BeyarR., et al., Influence of contractile state on curvilinearity of in situ end-systolic pressure-volume relations, *Circulation*, **79**, pp. 167-178, 1989.

[7] Claessens, T.E, Georgakopoulos, D., et al., Nonlinear isochrones in murine left ventricular pressure-volume loops: how well does the time-varying elastance concept hold?,*Am. J. Physiol Heart Circ. Physiol.*,**290**, pp. H1474-H1483, 2006.

[8] Sato, T., Shishido, T., et al., ESPVR of in situ rat left ventricle shows contractility-dependent curvilinearity, *Am. J. Physiol Heart Circ. Physiol.*,**274**, pp. H1429-H1434, 1998.

[9] ten Brinke, E.A., Klautz, R.J., Verwey, H.F., van der Wall, E.E., Dion, R.A., Steendijk, P., Single-beat estimation of the left ventricular end-systolic pressure-volume relationship in patients with heart failure*, Acta Physiol*., **198**, pp. 37-46, 2010.

[10] Kjorstad, K.E, Korvald, C, Myrmel T, Pressure-volume-based single-beat estimation cannot predict left ventricular contractility in vivo, *Am. J. Physiol Heart Circ. Physiol.*,**282**,pp. H1739-H1750, 2002.

[11] J.W. Burns, J.W. Covell, R. Myers, J. Ross Jr, Comparison of directly measured left ventricular wall stress and stress calculated from geometric reference figures, *Circ. Res.,***28**,pp. 611-621, 1971.